



---

## **IMPACT OF URBANIZATION ON URBAN HEAT ISLAND EFFECT BASED ON TM IMAGERY IN WUHAN, CHINA**

**Qijiao Xie<sup>1</sup>, Zhixiang Zhou<sup>2\*</sup>**

<sup>1</sup>School of Resources and Environmental Science, Hubei University, 430062 Wuhan, China

<sup>2</sup>College of Horticultural & Forestry Science/Key Laboratory of Horticultural Plant Biology (Ministry of Education), Huazhong Agricultural University, 430070 Wuhan, China

---

### **Abstract**

As natural landscapes are increasingly replaced by impervious surface materials associated with urbanization, urban areas tend to experience higher surface temperatures when compared to rural areas, which is known as the urban heat island (UHI) effect. In this study the impact of urbanization on land surface temperature (LST) and the UHI effect were examined based on two Landsat Thematic Mapper (TM) imageries of 1987 and 2007. Results show that Wuhan experienced rapid urban expansion from 1987 to 2007, while the areal extent with higher temperatures did not always correspond to the urbanized area. The percent impervious surface area (ISA) was found to efficiently explain the LST variation in urban areas, especially in high-density ones. The normalized difference vegetation index (NDVI) was a sufficient indicator to express surface temperature variation only in natural context. These findings help urban planners and greening designers make appropriate decisions on urban planning and thermal management.

**Key words:** impervious surface area, land surface temperature, normalized difference vegetation index, remote sensing, urban thermal environment

*Received: March, 2012; Revised final: April, 2013; Accepted: May, 2013*

---

### **1. Introduction**

One of the environmental consequences of urbanization and industrialization is the urban heat island (UHI) effect, a phenomenon of higher atmospheric and surface temperatures occurring in urban areas than in surrounding rural areas (Gluch et al., 2006; Voogt and Oke, 2003). Higher urban temperatures generally result in adverse economic and environmental impacts locally, regionally and globally. Persistent higher temperatures increase the demand for air conditioning, raise pollution levels, change urban thermal environments and ultimately lead to thermal discomforts and incidence of heat-related illnesses.

The UHI effect is essentially a thermal pollution caused by human activity and regarded as a

powerful force in local climate change (Du et al., 2007; Luber and McGeehin, 2008; Zheng et al., 2014). With the rapid increase of population and buildings in urban areas, anthropogenic waste heat released from vehicles, air conditioners, power plants and industries have steadily increased (Manea et al., 2013), which heats up the urban environment directly. Urban development can tremendously alter the urban surface structures by replacing natural landscapes with a large expanse of non-evaporating impervious surfaces such as concrete and asphalt (Oke, 1982; Owen et al., 1998; Tang et al., 2014). Physical change of the urban surface (albedo, thermal capacity, heat conductivity) can affect urban surface temperatures by altering the sensible and latent heat exchange between the urban surface and boundary layers (Frey and Parlow, 2012; Mohan and Kandya,

---

\* Author to whom all correspondence should be addressed: e-mail: whzhouzx@mail.hzau.edu.cn; Phone: +86-27-87284232; Fax: +86-27-87282010

2015). The land surface temperature (LST) will unavoidably propagate both downward into the subsurface (Baker and Baker, 2002; Taniguchi et al., 2005) and upward into atmosphere (Brazel et al., 2007; Jin et al., 2011; Jones et al., 1990). Then surface, subsurface and air urban heat islands can be detected (Roth et al., 1989; Voogt and Oke, 2003).

Urbanization typically leads to the reduction of green spaces in urban areas, which modifies urban surface water content and vegetation cover (Owen et al., 1998). Research found that, with regard to the surface energy balance, latent heat exchange was dominant in more vegetated areas, while sensible heat exchange was dominant in impervious areas (Oke, 1982). This finding is attracting mounting attention on the relationship between LST and urban vegetation. Much emphasis has been placed on the relationship between LST and the normalized difference vegetation index (NDVI) (Gallo et al., 1993; Lo et al., 1997; Nonomura et al., 2009; Owen et al., 1998; Price, 1990; Raynolds et al., 2008) or other NDVI-related parameters, such as vegetation abundance (Gillies and Carlson, 1995; Lo et al., 1997; Weng, 2001) and vegetation fraction (Gutman and Ignatov, 1998; Weng et al., 2004). Results indicate that there is a negative correlation between LST and NDVI, which is valuable for UHI and urban climate studies.

On the other hand, much attention was paid on land cover changes associated with urbanization and their impact on LST (Fabrizi et al., 2010; Hamdi, 2010; Liu and Zhang, 2011; Xiong et al., 2012). The rapid changes of land use and land cover in urban areas result in the increase of impervious surface areas (ISA) in urban area. Because the amount of ISA is closely related to population growth and urban expansion, it was used to quantify the degree of urbanization and extent of urban land use (Carlson, 2012; Civco et al., 2002; Essa et al., 2013; Lynn et al., 2009; Xian and Crane, 2006; Yang et al., 2003; Yuan and Bauer, 2007) and indicate the environmental quality (Arnold and Gibbons, 1996; Xiao et al., 2007). Increased concern has been directed to the comparative studies of NDVI and percent ISA as indicators of surface urban heat island effect based on Landsat imagery by investigating the relationships between the LST, percent ISA and the NDVI (Deng and Wu, 2013; Ma et al., 2010; Yuan and Bauer, 2007; Zhang et al., 2009). Compared to the NDVI, the percent ISA was found to be more stable and less affected by seasonal changes in urbanized environment. Therefore, it is important to analyze the relationship between the LST and percent ISA in urban areas, for it provides an effective method to study urban expansion and related UHI effect.

LST is useful to predict the energy and water exchanges between land surface and atmosphere, which plays an important role in human–environment interactions. Urban expansion and development and their adverse effect on urban thermal environment has been confirmed by analyzing the relationship

between LST, NDVI and percent ISA in past literatures. However, further investigation on the correlation between LST and NDVI at different levels of urban development is necessary. This study aims to examine the urban expansion and its impact on urban surface temperatures and the surface UHI effect and also to analyze the varied efficiency of vegetation on reducing surface temperatures in different urban developed areas. The ultimate goal is to provide a better understanding of the relationship between LST, NDVI and percent ISA, and allow urban planners and managers to control and manage the urbanization and associated thermal pollution.

## 2. Case studies

### 2.1. Study area description

The study area is Wuhan city, located at  $113^{\circ}41' \sim 115^{\circ}05'E$ ,  $29^{\circ}58' \sim 31^{\circ}22'N$ . Wuhan is the capital of Hubei province, situated at the center of central China and in eastern Hubei, where the Yangtze River joins the Han River. It covers an area of over  $8000\text{ km}^2$ , with a population of more than 8 million. It has a long history of more than 3500 years. It is an economic center and an important transportation pivot of China. The metropolitan area comprises three parts: Wuchang, Hankou and Hanyang, commonly called Three Towns of Wuhan. These three parts face each other across the rivers and are linked by bridges.

Wuhan is situated in the north-subtropical climatic zone with four distinctive seasons. Spring and autumn are generally mild, while winter is cool with occasional snow. Due to its oppressively hot and humid summers, Wuhan is commonly known as one of the Three Furnaces of China, along with Nanjing and Chongqing. The annual temperature is  $15.8^{\circ}\text{C}$  to  $17.5^{\circ}\text{C}$  with extreme temperatures ranging from  $-18.1^{\circ}\text{C}$  to  $42.0^{\circ}\text{C}$ . The annual average precipitation is 1269 mm, concentrated during June to August. The annual frost free period lasts 211 to 272 days and annual sunlight duration is 1810 to 2100 hours.

### 2.2. Derivation of LST, NDVI and related indexes from Landsat TM imageries

LST data were derived from the thermal infrared (TIR) band (band6) of the radiometrically and geometrically corrected images (Voogt and Oke, 2003), which was conducted in Erdas Imagine 9.2 with several procedures: radiometric calibration, at-satellite temperature calculation, emissivity correction and LST estimation. In this study, we used two Landsat-5 Thematic Mapper (TM) images acquired on September 26, 1987 and April 10, 2007. At first, the DN value of Landsat TM band6 was converted into spectral radiance (Chander and Markham, 2003). The spectral radiance was then converted into at-satellite temperature (i.e., blackbody temperature or brightness temperature) under the assumption of uniform emissivity. The at-

satellite temperature obtained was referenced to a black body and not the real surface temperature. Therefore, emissivity corrections became necessary according to the nature of land cover when calculating LST. Built-up and bare land areas were assigned an emissivity value of 0.923 and water 0.9925 (Gong et al., 2005; Masuda et al., 1988). Emissivity of vegetated areas was modeled with the NDVI values through field measurement (Van De Griend and Owe, 1993). Then the emissivity corrected LST was computed (Artis and Carnahan, 1982).

Vegetation abundance has been identified as an important parameter to positively mitigate the UHI effect, which can be indicated through NDVI value. Together with the other two indexes: normalized difference built-up index (NDBI) and modified normalized difference water index (MNDWI), the NDVI value can be accurately calculated based on the spectral reflectances accordingly (Chander and Markham, 2003; Chander et al., 2009).

### 2.3. Water extraction

A great number of studies have stated that there exists a positive correlation between NDVI and LST in water bodies (Rinner and Hussain, 2011; Zášek and Oštir, 2012). In this study, water area accounts for a large percentage, which would significantly debase the accuracy of the relationship between vegetation and LST. Thus it is important to exclude the water body from the images before quantitatively and statistically analyzing the relationships between LST and NDVI. The MNDWI was used to extract and exclude the water bodies with the appropriate threshold values.

### 2.4. Derivation of urban percent ISA

The urban percent of impervious surface area (ISA) was highly correlated with urban land use/land cover types and the spatial distribution patterns (Jennings et al., 2004; Xian and Crane, 2005). For rural areas, the relationship between the urban percent ISA and NDBI was used to obtain the percent ISA through thresholding the NDBI value (Zhang et al., 2009).

For built up areas, Ridd (1995) found a strong negative correlation between ISA and fractional vegetation cover. Choudhury et al. (1994) and Carlson and Ripley (1997) then quantified the relationship between the percent ISA and fractional vegetation cover based on NDVI value by the Eq. (1), where:  $NDVI_{soil}$  and  $NDVI_{veg}$  are the NDVI values of the pixels covered by soil or non-vegetation and full vegetation.

$$ISA = 1 - \left( \frac{NDVI - NDVI_{soil}}{NDVI_{veg} - NDVI_{soil}} \right)^2 \quad (1)$$

## 3. Results

### 3.1. Spatial pattern of the percent ISA

In this study, the percent ISA was used to indicate the extent of the urban expansion and the level of urban development. Fig. 1 illustrates the spatial distribution patterns of the percent ISA continuously ranging from 0– 100%. Increasing values from natural landscape (such as green spaces and water bodies) to the built-up areas were found in both 1987 and 2007. The white color representing higher percent ISA values captured the central business districts (CBD), urban residential areas and major highways. Though the spatial patterns of percent ISA for 1987 and 2007 seemed similar, the spatial areal extent significantly varied. The area with higher percent ISA values has remarkably expanded from 1987 to 2007, with the sprawling trend of impervious surface mainly occurring around the urban core and along the major roads.

To quantify the changes in the urban development, ISA was classified into different categories by threshold values: less than 10% as non-urban (such as forest, water and park in city), 10-45% as low-density, 45-80% as medium-density and more than 80% as high-density urban areas. This classification of land-cover types involved the urban built-up areas, rural developed centers and relatively undeveloped rural areas. Detailed information on spatial extent and area change of different categories of percent ISA from 1987 to 2007 is described in Table 1. From this table, it is obvious that there has been a drastic change in urban built-up areas over this period. The areas of medium-density (45-80% ISA) and high-density (> 80% ISA) were 112.80 km<sup>2</sup> and 174.67 km<sup>2</sup> in 1987, significantly increasing to 591.45 km<sup>2</sup> and 560.69 km<sup>2</sup> respectively in 2007. The wide variation between 1987 and 2007 revealed that the city has experienced rapid urban expansion during the last two decades

### 3.2. Spatial pattern of LST

Fig. 2 shows the spatial distribution of land surface temperatures derived from TM image acquired on September 26, 1987 (a) and April 10, 2007 (b) in Wuhan City. The mean summer LST of 1987 was 39.6°C (SD of 4.7°C) with the lowest one 29.7 °C occurring in water and the highest one 62.8°C appearing in built-up area (Fig. 2a), while the mean late spring LST of 2007 was 22.4°C (SD of 3.8°C) with the lowest one 12.3 °C in water and the highest one 35.7°C in farmland (Fig. 2b). From the thermal maps, not only the spatial patterns of LST but also the urban heat island effect could be detected. The higher-grade highway running through the city created interlaced ‘hot channels’. Contrastively, the Yangtze River together with other water bodies had relatively lower temperatures, which produced a ‘cool corridor’ flowing through the city.

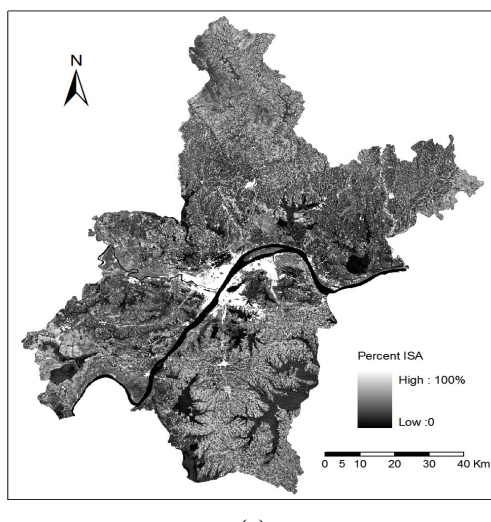
### 3.3. Relationship between percent ISA and LST

Table 2 presents the mean and standard deviation (SD) of LST for different categories of percent ISA. It is obvious that for both 1987 and 2007, the high-density type (>80% ISA) exhibits the highest LST as compared to other land cover types. Difference of the mean LST values between the relatively developed areas (>10% ISA) and rural areas (<10% ISA) means the UHI effect definitely exists in the study area. The largest difference naturally occurred between high-density urban area (>80% ISA) and rural areas (< 10% ISA) both for 1987 (12.27°C) and 2007 (5.66°C). The UHI intensity in different density urban areas (Table 2) in 1987 was larger than that in 2007, probably because the mean LST values were expected to be more

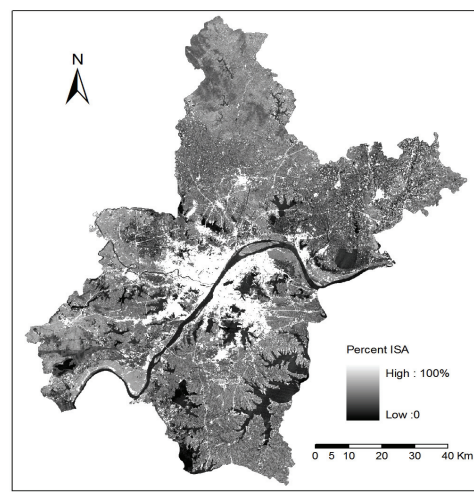
variable and heterogeneous over the study region in summer (1987) than in late spring (2007). The SD of LST for different categories of percent ISA (Table 2), with higher SD values in 1987 than in 2007, further supports this conclusion.

To quantify the relationship between percent ISA and the mean LST, a zonal analysis was carried out to evaluate the mean LST at each 1% increment of percent ISA from 0% to 100%. Fig. 3a and b show a relatively strong linear relationship ( $R^2=0.428$ ) between percent ISA and the mean LST for 1987 and a weak one ( $R^2=0.056$ ) for 2007.

However, the shapes seemed similar in both cases, indicating linear increasing trends in the rural areas (<10% ISA) and urban developed areas (>45% ISA) and a linear decreasing one in the suburbs (approximately 20-45%ISA).

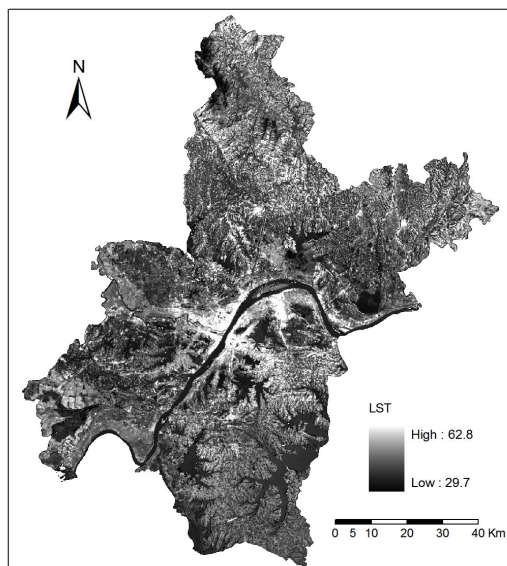


(a)

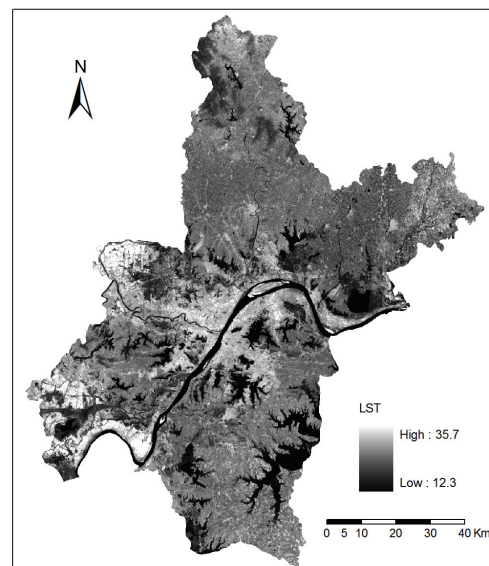


(b)

**Fig. 1.** Spatial distribution patterns of percent impervious surface area (ISA) from TM images acquired on September 26, 1987 (a) and April 10, 2007 (b)



(a)



(b)

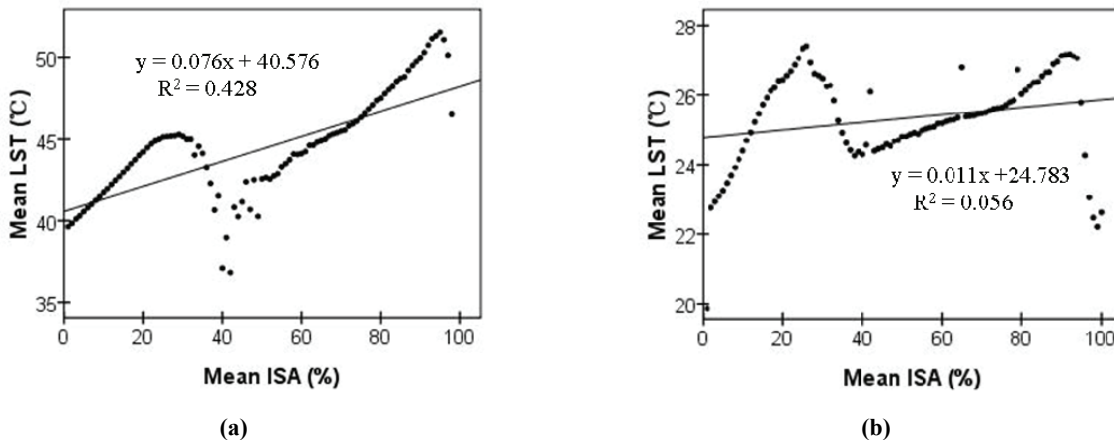
**Fig. 2.** Spatial distribution patterns of land surface temperature (LST) derived from TM images acquired on September 26, 1987 (a) and April 10, 2007 (b)

**Table 1.** Change in area from 1987 to 2007 of different categories of percent ISA

Year/Percent ISA	<10% ISA	10%-45% ISA	45%-80% ISA	>80% ISA
1987 ( $\text{km}^2$ )	5883.72	2240.81	112.80	174.67
2007 ( $\text{km}^2$ )	5927.55	1418.96	591.45	560.69
Difference ( $\text{km}^2$ )	43.83	-821.85	478.65	386.02
Percent change (%)	0.74	-36.68	424.34	221.00

**Table 2.** Mean LST in different levels of urban development for 1987 and 2007

Year/Percent ISA	<10% ISA	10%-45% ISA	45%-80% ISA	>85% ISA
Mean LST of 1987 ( $^{\circ}\text{C}$ )	36.96	43.20	45.34	49.23
SD of 1987 ( $^{\circ}\text{C}$ )	6.42	4.81	5.69	4.08
Mean LST of 2007 ( $^{\circ}\text{C}$ )	20.96	25.47	25.77	26.62
SD of 2007 ( $^{\circ}\text{C}$ )	3.46	2.66	1.45	1.68

**Fig. 3.** Relationship of mean land surface temperature (LST) to percent impervious surface area (ISA): (a) 1987, (b) 2007

### 3.4. Relationship between LST and NDVI for different urban development density

To quantitatively investigate the relationship between the NDVI and the mean LST for each category of percent ISA, a zonal analysis was carried out to account for the mean LST at each 0.01 increment of NDVI from 0 to 1 (with water excluded). Fig. 4 shows their linear regression correlations. The highest negative correlation coefficient was found in non-urban areas (<10% ISA) for both 1987 ( $R^2=0.753$ ) and 2007 ( $R^2=0.953$ ). This stronger negative correlation between LST and NDVI imply that NDVI in more vegetated areas (<10% ISA) can better explain surface temperature variations than that in sparsely vegetated areas (>10% ISA).

The correlation coefficients in the other three urban areas (>10% ISA) complied with the orders: high-density (0.669) > low-density (0.397) > medium-density (0.201) for 1987 and medium-density (0.681) > low-density (0.545) > high-density (0.351) for 2007. Results show that LST values tend to negatively correlate with NDVI values in different urban development density areas in both years. The negative correlation illustrates the importance of urban vegetation in reducing urban surface temperatures. The specified effects of NDVI on cooling surface temperature significantly varied in different development density areas in both years

(shown in Fig. 4). This coefficient variation at different urban development levels between the two years indicates that the correlation of NDVI and LST can be influenced by many factors, such as land cover diversity, landscape heterogeneity and environmental complexity in urban areas.

## 4. Discussions

In this study, the percent ISA was selected to quantitatively represent urbanization level in Wuhan. What attracted our attention was that the degree of urbanization was defined by thresholding the values of the percent ISA. Nevertheless, the thresholds were subjectively assigned, with no unified standards. This diversity of threshold values prevented the urbanization degrees of different studied areas from being comparable.

When masking the spatial distributions of percent ISA (Fig. 1) over the corresponding LST maps (Fig. 2) for 1987 and 2007, a noticeable result appeared. The areal extent with higher temperatures did not always correspond to the urbanized area, though there was an ongoing expansion in built-up areas from 1987 to 2007.

This differs from the previous researches (Liu and Zhang, 2011; Rinner and Hussain, 2011; Xiong et al., 2012), which indicated that the UHI spatial distributions was mainly restricted to urbanized or industrialized areas.

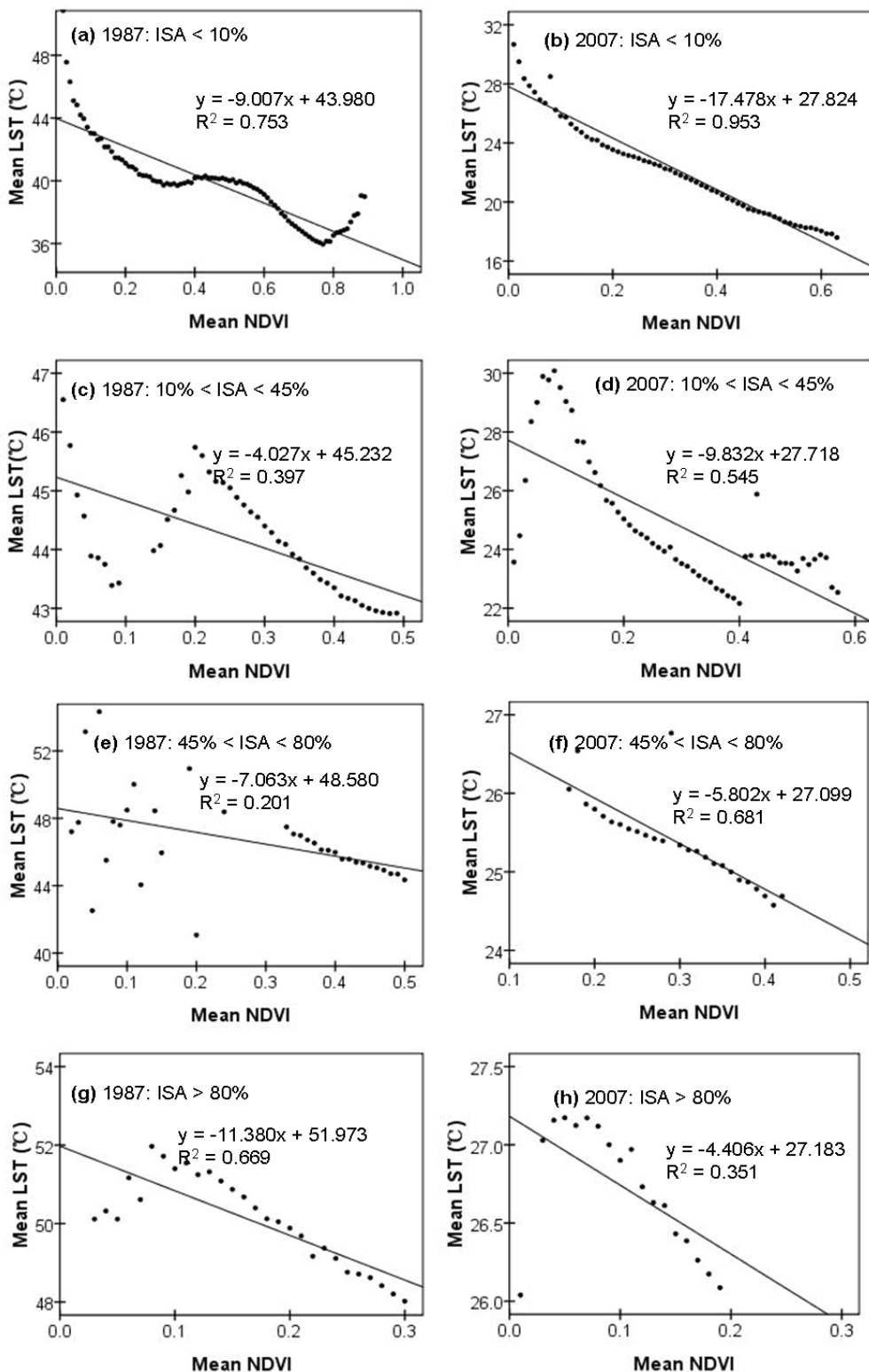


**Fig. 4.** Relationship of mean land surface temperature (LST) in  $^{\circ}\text{C}$  to normalized difference vegetation index (NDVI) at different urban development levels (percent ISA)

Specifically, in this study, in addition to the UHI areas dominated by residential buildings, commercial areas and industrial areas in 1987 as well as in 2007 (Fig. 2a and b), another obvious heat island was found in the southwest of the city in 2007 (Fig. 2b). This is, at least in part, because the

farmlands accounted for a large percentage in the southwest and they seasonally varied in vegetation cover due to agricultural activities. They were fully covered by crops with high vegetation cover and great green biomass in summer (1987) but remained nearly fallow and bare in late spring (2007). Bare soil

was found to be similar in thermal response to impervious surface (Gluch et al., 2006; Huang et al., 2008). It is worth noting that the linear relationship between the mean LST and percent ISA in this study (Fig.3) is much weaker than those in the literatures (Yuan and Bauer, 2007; Zhang et al., 2009).

The reason is that the previous researches were conducted in relatively homogeneous urban areas, while our study in the areas with natural and impervious surface mixed. The context heterogeneity, to some extent, influenced the explanation quality of the percent ISA on LST. Remarkably, a decreasing trend was detected in the low-density urban areas due to the mixed and complex surface covers. This partly weakened the general linear relationship between percent ISA and LST.

The similar varying temperature trends to different categories of percent ISA in the two observed years are shown in Fig.3, which implied that the mean LST can be well explained by percent ISA in homogeneously covered areas. On the other hand, relatively steeper slope of linear correlation was detected in summer image than that in spring one, indicating that higher UHI magnitude appeared in summer. It is due to seasonal thermal performance associated with varied surface covers. Significant sensible heat exchange occurs mainly in areas with sparse or no vegetation cover and latent heat fluxes represent in areas characterized by vegetation cover (Lo et al., 1997). Impervious surface in urban areas expressed relatively higher warming rate in summer and higher efficiency of surface heat release in spring or winter than natural surface did (Yuan and Bauer, 2007; Yang et al., 2010).

NDVI is usually used as a parameter to indicate the biomass, percentage cover and abundance of urban vegetation (Lo et al., 1997). The NDVI value ranges generally from -1 to 1. Normally, it is positive in vegetated area, close to zero for impervious surface and negative for water bodies (Van De Griend and Owe, 1993). Typically, higher NDVI values indicate a larger amount of vegetation cover and express lower temperatures in pixels. In this study, the relationships between NDVI and LST were confirmed to be nonlinear in all categories of percent ISA except for in non-urban areas (<10% ISA).

That is to say, sparsely vegetated areas experience a wider variation in LST than densely vegetated ones (Owen et al., 1998; Price, 1990). This suggests that NDVI can be a sufficient indication to express surface temperature variation only in natural context.

## 5. Conclusions

Anthropogenic activities associated with urbanization and industrialization were the most important driving force in land cover changes and UHI formation, as expected. Agricultural activity was another artificial factor contributing to the

seasonal variation of land covers and land surface temperatures.

The percent ISA was suitable for LST studies in urbanized areas and NDVI was sufficient to express surface temperature variation in vegetated areas. What has yet to be examined is how to select appropriate threshold values of the percent ISA to define urbanization degree. Future studies need to focus on better understanding the seasonal influence on the relationship between NDVI, percent ISA and LST variation.

## Acknowledgments

This research was sponsored by the National Science and Technology Supporting Program (No. 2013BAJ02B01), the National Natural Science Foundation of China (Grant No. 41401186), the Natural Science Foundation of Hubei Province of China (2014CFB346), the Fund No. 200951999569 and the Program No. 2013PY133. The authors would like to thank Elizabeth Lord from the University of Toronto, Canada for reviewing and correcting the paper. We are also grateful to the Editor and the anonymous referees for their helpful comments and suggestions.

## References

- Arnold C.L., Gibbons C.J., (1996), Impervious surface coverage: The emergence of a key environmental indicator, *Journal of the American Planning Association*, **62**, 243-258.
- Artis D.A., Carnahan W.H., (1982), Survey of emissivity variability in thermography of urban areas, *Remote Sensing of Environment*, **12**, 313-329.
- Baker J.M., Baker D.G., (2002), Long-term ground heat flux and heat storage at a mid-latitude site, *Climate Change*, **54**, 295-303.
- Brazel A., Gober P., Lee S.J., Grossman-Clarke S., Zehnder J., Hedquist B., (2007), Determinants of changes in the regional urban heat island in metropolitan Phoenix (Arizona, USA) between 1990 and 2004, *Climate Research*, **33**, 171-82.
- Carlson T.N., Ripley D.A., (1997), On the relation between NDVI, fractional vegetation cover, and leaf area index, *Remote Sensing of Environment*, **62**, 241-252.
- Carlson T.N., (2012), Land use and impervious surface area by county in Pennsylvania (1985-2000) as interpreted quantitatively by means of satellite imagery, *The Open Geography Journal*, **5**, 59-67.
- Chander G., Markham B., (2003), Revised Landsat-5 TM radiometric calibration procedures and postcalibration dynamic ranges, *IEEE Transactions on Geoscience and Remote Sensing*, **41**, 2674-2677.
- Chander G., Markham B.L., Helder D.L., (2009), Summary of current radiometric calibration coefficients for Landsat MSS, TM, ETM+ and EO-1 ALI sensors, *Remote Sensing of Environment*, **113**, 893-903.
- Choudhury B.J., Ahmed N.U., Idso S.B., Reginato R.J., Daughtry C.S.T., (1994), Relations between evaporation coefficients and vegetation indices studied by model simulations, *Remote Sensing of Environment*, **50**, 1-17.
- Civco D.L., Hurd J.D., Wilson E.H., Arnold C.L., Prisloe Jr. M.P., (2002), Quantifying and describing urbanizing landscapes in the northeast United States, *Photogrammetric Engineering and Remote Sensing*, **68**, 1083-1090.

- Deng C.B., Wu C.S., (2013), Examining the impacts of urban biophysical compositions on surface urban heat island: A spectral unmixing and thermal mixing approach, *Remote Sensing of Environment*, **131**, 262-274.
- Du Y., Xie Z.Q., Zeng Y., Shi Y.F., Wu J.G., (2007), Impact of urban expansion on regional temperature change in the Yangtze River Delta, *Journal of Geographical Sciences*, **17**, 387-398.
- Essa W., van der Kwast J., Verbeiren B., Batelaan O., (2013), Downscaling of thermal images over urban areas using the land surface temperature–impervious percentage relationship, *International Journal of Applied Earth Observation and Geoinformation*, **23**, 95-108.
- Fabrizi R., Bonafoni S., Biondi R., (2010), Satellite and Ground-Based Sensors for the Urban Heat Island Analysis in the City of Rome, *Remote Sensing*, **2**, 1400-1415.
- Frey C.M., Parlow E., (2012), Flux measurements in Cairo. Part 2: On the determination of the spatial radiation and energy balance using ASTER satellite data, *Remote Sensing*, **4**, 2635-2660.
- Gallo K.P., McNab A.L., Karl T.R., Brown J.F., Hood J.J., Tarpley J.D., (1993), The use of NOAA AVHRR data for assessment of the urban heat island effect, *Journal of Applied Meteorology*, **32**, 899-908.
- Gillies R.R., Carlson T.N., (1995), Thermal remote sensing of surface soil water content with partial vegetation cover for incorporation into climate models, *Journal of Applied Meteorology*, **34**, 745-756.
- Gluch R., Quattrochi D.A., Luval J.C., (2006), A multi-scale approach to urban thermal analysis, *Remote Sensing of Environment*, **104**, 123-132.
- Gong A.D., Jiang Z.Y., Li J., Chen Y.H., Hu H.L., (2005), Urban land surface temperature retrieval based on landsat TM remote sensing images in Beijing, *Remote Sensing Information*, **3**, 18-20.
- Gutman G., Ignatov A., (1998), The derivation of the green vegetation fraction from NOAA/AVHRR data for use in numerical weather prediction models, *International Journal of Remote Sensing*, **19**, 1533-1543.
- Hamdi R., (2010), Estimating urban heat island effects on the temperature series of uccle (Brussels, Belgium) using remote sensing data and a land surface scheme, *Remote Sensing*, **2**, 2773-2784.
- Huang L.M., Li J.L., Zhao D.H., Zhu J.Y., (2008), A fieldwork study on the diurnal changes of urban microclimate in four types of ground cover and urban heat island of Nanjing, China, *Building and Environment*, **43**, 7-17.
- Jennings D.B., Jarnagin S.T., Ebert D.W., (2004), A modeling approach for estimating watershed impervious surface area from national land cover data 92, *Photogrammetric Engineering and Remote Sensing*, **70**, 1295-1307.
- Jin M.S., Kessomkiat W., Pereira G., (2011), Satellite-observed urbanization characters in Shanghai, China: aerosols, urban heat island effect, and land-atmosphere interactions, *Remote Sensing*, **3**, 83-99.
- Jones P.D., Groisman P.Y., Coughlan M., Plummer N., Wang W.C., Karl T.R., (1990), Assessment of urbanization effects in time-series of surface air-temperature over land, *Nature*, **347**, 169-72.
- Liu L., Zhang Y.Z., (2011), Urban heat island analysis using the landsat TM data and ASTER data: A case study in Hong Kong, *Remote Sensing*, **3**, 1535-1552.
- Lo C.P., Quattrochi D.A., Luval J.C., (1997), Application of high-resolution thermal infrared remote sensing and GIS to assess the urban heat island effect, *International Journal of Remote Sensing*, **18**, 287-304.
- Luber G., McGeehin M., (2008), Climate change and extreme heat events, *American Journal of Preventive Medicine*, **35**, 429-435.
- Lynn B.H., Carlson T.N., Rosenzweig C., Goldberg R., Drury L., Cox J., Gaffin S., Parshall L., Civerolo K., (2009), A modification of the NOAH LSM to simulate heat mitigation strategies in the New York City metropolitan area, *Journal of Applied Meteorology and Climatology*, **48**, 199-216.
- Ma Y., Kuang Y.Q., Huang N.S., (2010), Coupling urbanization analyses for studying urban thermal environment and its interplay with biophysical parameters based on TM/ETM+ imagery, *International Journal of Applied Earth Observation and Geoinformation*, **12**, 110-118.
- Manea D.L., Manea E.E., Robescu D.N., (2013), Study on greenhousegas emissions from wastewater treatment plants, *Environmental Engineering and Management Journal*, **12**, 59-63.
- Masuda K., Takashima T., Takayama Y., (1988), Emissivity of pure and sea waters for the model sea surface in the infrared window region, *Remote Sensing of Environment*, **24**, 313-332.
- Mohan M., Kandy A., (2015), Impact of urbanization and land-use/land-cover change on diurnal temperature range: A case study of tropical urban airshed of India using remote sensing data, *Science of the Total Environment*, **506-507**, 453-465.
- Nonomura A., Kitahara M., Masuda T., (2009), Impact of land use and land cover changes on the ambient temperature in a middle scale city, Takamatsu, in Southwest Japan, *Journal of Environmental Management*, **90**, 3297-3304.
- Oke T.R., (1982), The energetic basis of the urban heat island, *Quarterly Journal of the Royal Meteorological Society*, **108**, 1-24.
- Owen T.W., Carlson T.N., Gillies R.R., (1998), An assessment of satellite remotely-sensed land cover parameters in quantitatively describing the climatic effect of urbanization, *International Journal of Remote Sensing*, **19**, 1663-1681.
- Price J.C., (1990), Using spatial context in satellite data to infer regional scale evapotranspiration, *IEEE Transactions on Geoscience and Remote Sensing*, **28**, 940-948.
- Raynolds M.K., Comiso J.C., Walker D.A., Verbyla D., (2008), Relationship between satellite-derived land surface temperatures, arctic vegetation types, and NDVI, *Remote Sensing of Environment*, **112**, 1884-1894.
- Ridd M.K., (1995), Exploring a V-I-S (vegetation-impervious-surface-soil) model for urban ecosystem analysis through remote sensing: comparative anatomy for cities, *International Journal of Remote Sensing*, **16**, 2165-2185.
- Rinner, C.; Hussain, M., (2011), Toronto's Urban Heat Island—Exploring the Relationship between Land Use and Surface Temperature, *Remote Sensing*, **3**, 1251-1265.
- Roth M., Oke T.R., Emery W.J., (1989), Satellite-derived urban heat islands from three coastal cities and utilization of such data in urban climatology, *International Journal of Remote Sensing*, **10**, 1699-1720.

- Tang Z., Shi C.B., Bi K.X., (2014), Impacts of land cover change and socioeconomic development on ecosystem service values, *Environmental Engineering and Management Journal*, **13**, 2697-2705.
- Taniguchi M., Uemura T., Sakura Y., (2005), Effects of urbanization and groundwater flow on subsurface temperature in three megacities in Japan, *Journal of Geophysics and Engineering*, **2**, 320-5.
- Van De Griend A.A., Owe M., (1993), On the relationship between thermal emissivity and the normalized difference vegetation index for nature surfaces, *International Journal of Remote Sensing*, **14**, 1119-1131.
- Voogt J.A., Oke T.R., (2003), Thermal remote sensing of urban areas, *Remote Sensing of Environment*, **86**, 370-384.
- Weng Q., (2001), A remote sensing-GIS evaluation of urban expansion and its impact on surface temperature in the Zhujiang Delta, China, *International Journal of Remote Sensing*, **22**, 1999-2014.
- Weng Q.H., Lu D.S., Schubring J., (2004), Estimation of land surface temperature-vegetation abundance relationship for urban heat island studies, *Remote Sensing of Environment*, **89**, 467-483.
- Xian G., Crane M., (2005), Assessments of urban growth in the Tampa Bay watershed using remote sensing data, *Remote Sensing of Environment*, **97**, 203-215.
- Xian G., Crane M., (2006), An analysis of urban thermal characteristics and associated land cover in Tampa Bay and Las Vegas using Landsat satellite data, *Remote Sensing of Environment*, **104**, 147-156.
- Xiao R.B., OuYang Z.Y., Zheng H., Li W.F., Schienke E.W., Wang X.K., (2007), Spatial pattern of impervious surfaces and their impacts on land surface temperature in Beijing, China, *Journal of Environmental Sciences*, **19**, 250-256.
- Xiong Y.Z., Huang S.P., Chen F., Ye H., Wang H., Zhu C.B., (2012), The impacts of rapid urbanization on the thermal environment: a remote sensing study of Guangzhou, South China, *Remote Sensing*, **4**, 2033-2056.
- Yang L., Huang C., Homer C.G., Wylie B.K., Coan M.J., (2003), An approach for mapping large-area impervious surfaces: Synergistic use of Landsat 7 ETM+ and high spatial resolution imagery, *Canadian Journal of Remote Sensing*, **29**, 230-240.
- Yang S. B., Zhao X. Y., Shen S. H., Hai Y. L., Fang Y.X., (2010), Characteristics of urban heat island seasonal pattern in beijing based on landsat TM / ETM+ Imagery (in Chinese), *Transactions of Atmospheric Sciences*, **33**, 427-435.
- Yuan F., Bauer M.E., (2007), Comparison of impervious surface area and normalized difference vegetation index as indicators of surface urban heat island effects in Landsat imagery, *Remote Sensing of Environment*, **106**, 375-386.
- Zakšek K., Oštir K., (2012), Downscaling land surface temperature for urban heat island diurnal cycle analysis, *Remote Sensing of Environment*, **117**, 114-124.
- Zhang Y.S., Odeh Inakwu O.A., Han C.F., (2009), Bi-temporal characterization of land surface temperature in relation to impervious surface area, NDVI and NDBI, using a sub-pixel image analysis, *International Journal of Applied Earth Observation and Geoinformation*, **11**, 256-264.
- Zheng B.J., Myint S.W., Fan C., (2014), Spatial configuration of anthropogenic land cover impacts on urban warming, *Landscape and Urban Planning*, **130**, 104-111.